

Lignin depolymerisation by nickel supported layered-double hydroxide catalysts†

Cite this: *Green Chem.*, 2014, **16**, 824

Matthew R. Sturgeon,^{a,b} Marykate H. O'Brien,^{a,b} Peter N. Ciesielski,^c Rui Katahira,^a Jacob S. Kruger,^a Stephen C. Chmely,^{‡a} Jessica Hamlin,^{a,b} Kelsey Lawrence,^{a,b} Glendon B. Hunsinger,^a Thomas D. Foust,^{a,b} Robert M. Baldwin,^{a,b} Mary J. Bidy*^{a,b} and Gregg T. Beckham*^{a,b}

Lignin depolymerisation is traditionally facilitated with homogeneous acid or alkaline catalysts. Given the effectiveness of homogeneous basic catalysts for lignin depolymerisation, here, heterogeneous solid-base catalysts are screened for C–O bond cleavage using a model compound that exhibits a common aryl–ether linkage in lignin. Hydrotalcite (HTC), a layered double hydroxide (LDH), is used as a support material as it readily harbours hydroxide anions in the brucite-like layers, which are hypothesised to participate in catalysis. A 5 wt% Ni/HTC catalyst is particularly effective at C–O bond cleavage of a model dimer at 270 °C without nickel reduction, yielding products from C–O bond cleavage identical to those derived from a base-catalysed mechanism. The 5% Ni-HTC catalyst is shown to depolymerise two types of biomass-derived lignin, namely Organosolv and ball-milled lignin, which produces alkyl-aromatic products. X-ray photoelectron spectroscopy and energy dispersive X-ray spectroscopy show that the nickel is well dispersed and converts to a mixed valence nickel oxide upon loading onto the HTC support. The structure of the catalyst was characterised by scanning and transmission electron microscopy and X-ray diffraction, which demonstrates partial dehydration upon reaction, concomitant with a base-catalysed mechanism employing hydroxide for C–O bond cleavage. However, the reaction does not alter the overall catalyst microstructure, and nickel does not appreciably leach from the catalyst. This study demonstrates that nickel oxide on a solid-basic support can function as an effective lignin depolymerisation catalyst without the need for external hydrogen and reduced metal, and suggests that LDHs offer a novel, active support in multifunctional catalyst applications.

Received 16th October 2013,
Accepted 7th November 2013

DOI: 10.1039/c3gc42138d

www.rsc.org/greenchem

Introduction

Lignin is a heterogeneous alkyl-aromatic polymer that can comprise up to 30–40% of the plant cell wall by mass, depending on the plant type. Its primary functions in nature are for structure, water transport, and defence against pathogens.¹ During cell wall biosynthesis, it is thought that lignin is polymerised *via* radical coupling reactions from three monomeric units: *p*-coumaryl alcohol (H), coniferyl alcohol (G), and sinapyl alcohol (S), which exhibit different degrees of ring

methoxy-substituents.^{1–4} The presence of three monomers with variable molecular connectivity imparts an inherently heterogeneous structure to lignin, resulting in a variety of C–O and C–C inter-monomer bonds with varying reactivity and bond strengths.^{5–7} Due to its heterogeneous structure and reactivity, production of fuels and chemicals from lignin has been technically challenging relative to carbohydrate utilisation to date. As such, most conversion processes to produce fuels and chemicals from lignocellulosic biomass typically slate the residual lignin component for combustion to produce process heat and power.^{8,9} A primary technical hurdle in lignin utilisation stems from the need to develop robust catalysts for lignin depolymerisation to low molecular weight species that can be fractionated and catalytically upgraded.

Over many decades of research and development, the pulp and paper industry has developed industrial processes for removing lignin from whole biomass based on homogeneous acid and alkaline catalysts, such as the Kraft, soda, and sulphite pulping processes. These approaches typically remove lignin in a liquor phase, which is also then burned for heat

^aNational Bioenergy Center, National Renewable Energy Laboratory, Golden, Colorado, USA. E-mail: gregg.beckham@nrel.gov, mary.bidy@nrel.gov; Fax: +1-303-384-6363; Tel: +1-303-384-7806

^bNational Advanced Biofuels Consortium, National Renewable Energy Laboratory, Golden, Colorado, USA

^cBiosciences Center, National Renewable Energy Laboratory, Golden, Colorado, USA

†Electronic supplementary information (ESI) available: Table S1. See DOI: 10.1039/c3gc42138d

‡Current address: Center for Renewable Carbon, University of Tennessee Institute of Agriculture, Knoxville, Tennessee, USA.

and power. Utilising a higher severity approach relative to pulping, several efforts have focused on base catalysed depolymerisation (BCD) of isolated lignin. In a series of seminal studies, Shabtai *et al.* examined the use of sodium hydroxide as a homogeneous alkaline catalyst in supercritical alcohols to depolymerise lignin. Therein, they demonstrated upwards of 95% conversion to primarily monomeric aromatic species with some oligomers present at 250–290 °C.^{10–14} Following BCD, the resulting stream could then be upgraded by ring hydrogenation and hydrocracking techniques to value-added molecules.¹⁵ Similarly, Miller *et al.* studied the use of mixed liquid hydroxides for lignin depolymerisation.¹⁶ They reported that KOH in supercritical ethanol at 290 °C will rapidly depolymerise both Kraft- and Organosolv-derived lignin in as little as 10 min with only 7% insoluble material remaining. More recently, Roberts *et al.* demonstrated that the base-catalysed deconstruction products from Organosolv lignin vary with process temperature in aqueous NaOH.¹⁷ They reported that monomer selectivity is a maximum between at 260 to 280 °C. While aqueous phase BCD shows promise for lignin depolymerisation, recovery and recycle of the homogeneous base catalyst is extremely difficult, especially given the heterogeneous composition and molecular weight of the products.

In addition to soluble, homogeneous alkaline catalysts, several recent studies have examined the use of homogeneous metal catalysts for aryl–ether bond cleavage in model systems including ruthenium,^{18–20} vanadium,^{21–23} cobalt,^{24–27} and nickel.^{28,29} These studies present elegant approaches and offer a significant level of understanding of C–O bond cleavage mechanisms. However, homogeneous catalysts may have more limited applicability relative to heterogeneous catalysts for lignin depolymerisation in an integrated biorefinery context.

To date, several metal-supported heterogeneous catalysts have been examined for lignin depolymerisation on substrates ranging from model compounds to biomass-derived lignin.^{30,31} For reductive depolymerisation strategies, these catalysts typically require high pressures of external hydrogen and reduced metals. Parsell *et al.* utilised a bimetallic Zn/Pd/C catalyst for aryl–ether bond cleavage with a model compound, guaiacylglycerol- β -guaiacyl ether, which was found to undergo complete conversion at 150 °C in methanol after 2 h under 300 psi of H₂.³² Wang and Rinaldi showed that RANEY® nickel is quite active (>99% conversion) in the cleavage of diphenyl ether in aprotic nonpolar solvents at 90 °C for 2.5 h under 725 psi H₂.³³ Hartwig and co-workers reported a ligand-less heterogeneous nickel catalyst to be active in the cleavage of diphenyl ether as well, also in the presence of H₂.³⁴ Towards demonstration of lignin depolymerisation on biomass-derived lignin, several different heterogeneous catalysts (supported Co, Pd, and Ni–Mo) have been reported to be active in lignin depolymerisation under H₂ at temperatures near 400 °C.^{35–38} Of particular note, Ni–Mo on a Cr₂O₃-support exhibited a high extent of lignin depolymerisation (80% liquid fraction) with <2% char under 2030 psi of H₂.³⁷ In a recent study Song *et al.* reported that Ni/C is active in the depolymerisation of birch

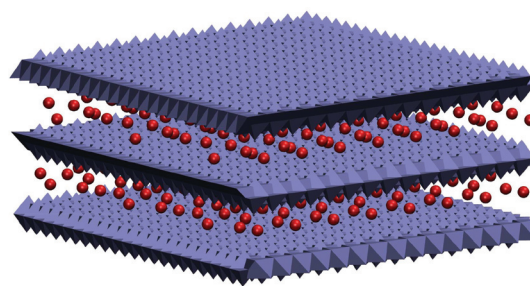


Fig. 1 Illustration of a layered double hydroxide, hydrotalcite, with hydroxide anions (red spheres) in the interstitial layer. The brucite-like layers are shown in purple. It is hypothesised here that the hydroxide anions may provide catalytic activity in the depolymerisation of lignin.

lignin in methanol at 200 °C for 6 h under Ar resulting in a 54% lignin conversion.³⁹ Taken together, these recent studies demonstrate that heterogeneous supported catalysts with reduced metals such as nickel under hydrogen pressure or in hydrogen-donor solvents show promise for lignin depolymerisation. To date, there has been less work to our knowledge on lignin depolymerisation on solid catalysts that do not require external hydrogen.

Inspired by the significant body of work on homogeneous alkaline depolymerisation of lignin,^{10–17} the advantages of heterogeneous catalysts for lignin depolymerisation,^{40,41} and the desire to utilise catalysts that do not require external hydrogen or reduced metals, catalyst supports that exhibit alkaline character are employed here as a starting point for catalyst design. Specifically, layered double hydroxides (LDHs) are low cost materials that can be obtained from abundantly available minerals.⁴² Unlike many clay minerals that exhibit negatively charged layers with cations in the interstitial layers, LDHs are ionic, lamellar materials with positively charged, brucite-like layers and interstitial anions, as illustrated in Fig. 1. These materials offer significant breadth of available chemistries as both the metals in the brucite-like layers and the anions in the interstitial layers are readily tuneable, and multiple LDHs are available naturally with a wide range of metals present.⁴² Thus, the range of potential catalytic applications available with LDHs, either directly as catalysts or as active supports in multifunctional catalysts, as well as the range of possible substrates given the ability to tune the interlayer spacing with different anions, suggests a significant potential for these materials as multifunctional catalyst materials.⁴² Moreover, LDHs and especially their metal oxide derivatives are stable in water and many organic solvents, reasonably thermally stable, and are readily regenerated, thus lending more support to potential broader application areas.⁴² To date, naturally occurring LDHs have been employed with interlayer hydroxide ions in base-catalysed reactions without substantial modification from the natural LDH composition, such as for aldol condensation and esterification.^{42–54} Hydrotalcite (HTC), Mg₆Al₂(OH)₁₆(CO₃)·4H₂O, represents a specific type of LDH that exhibits a well-defined structure (Fig. 1), which has also been used as a support in the synthesis of metal-supported catalysts for

various reforming, hydrogenation, and isomerisation reactions.^{55–63}

Here, it is hypothesised that nickel supported on HTC can depolymerise lignin *via* a base-catalysed mechanism mediated by a strong interaction between the ether oxygen and the nickel metal. To test this hypothesis, a library of nickel-loaded HTC catalysts is synthesised and screened for activity in the deconstruction of a lignin model compound containing a β -O-4 aryl-ether bond, namely 2-phenoxy-1-phenethanol (PE). PE has been extensively used as a model compound in studies aimed at understanding catalyst mechanisms.^{18–20,64} Additionally, the bond strength in PE has been shown to be similar to that in other dimers that exhibit the β -O-4 linkage with quantum mechanical calculations.⁵ A 5 wt% Ni/HTC catalyst is found to be the most active catalyst in the aryl-ether bond cleavage for the lignin model compound, and detailed catalytic characterisations are conducted with this material. Upon loading, Ni(NO₃)₂ converts primarily to Ni(OH)₂ on the HTC support; the nickel is retained in hot water washes and does not leach during the reactions conducted here. A single catalysis run at 270 °C converts most of the Ni(OH)₂ to a mixed valence nickel oxide, which is also shown to be an equivalently active catalytic species, yielding the same products in catalysis of the model compound. Notably, the 5 wt% Ni/HTC catalyst is demonstrated to deconstruct biomass-derived Organosolv lignin and ball-milled lignin, both isolated from corn stover, at 270 °C yielding significant amounts of low-molecular weight species identified by GC/MS relative to non-catalysed thermal treatment based on gel-permeation chromatography (GPC) measurements.

Results

Catalyst synthesis

Nickel-supported HTC was synthesised using wet impregnation, wherein Ni(NO₃)₂·6H₂O dissolved in ethanol was directly loaded onto commercial HTC. Three catalysts were initially synthesised at nickel loadings of 1.0, 5.0, and 11.0 wt% for screening purposes. Common post synthesis modifications of supported nickel catalysts often include calcination and reduction.^{65,66} Thus, two additional modified catalysts were

synthesised and screened: 5 wt% Ni/HTC was calcined at 300 °C in air and a sample of 5 wt% Ni/HTC was reduced under 5% H₂ (He balance) at 250 °C for 2.5 h. Further details on the methods employed in catalyst synthesis can be found in the Experimental methods section.

Catalyst activity screening

Catalytic activity was first screened on the lignin model compound 2-phenoxy-1-phenethanol (PE), shown in Fig. 2. PE is a representative lignin model compound containing a β -O-4 alkyl-aryl-ether bond, which is the most abundant inter-monomer bond in native lignin. A temperature of 270 °C was used for the initial catalyst screening. Methyl isobutyl ketone (MIBK) was used as the reaction solvent as it is a typical co-solvent used to fractionate biomass into its primary components in Organosolv processes.⁶⁷ For each reaction, the catalyst of interest and a stock solution of PE dissolved in MIBK were loaded into a 3 mL stainless steel batch reactor at a loading of 2 : 1 wt : wt, which correlates to a Ni : PE mass ratio = 0.1. Unless otherwise noted, catalysts were used as prepared without post synthesis modifications. The reactions were run at 270 °C for 1 hour in triplicate. The reaction mixture was washed from the reactor with a known amount of acetone and the catalyst was removed. Further details regarding the experimental conditions and procedures are described in the Experimental methods section. In all cases, PE was converted to phenol and acetophenone (1-phenylethanone) by base-catalysed cleavage of the β -O-4 aryl-ether bond (Fig. 2). The resulting solution was analysed by gas chromatography for concentration of PE, phenol, and acetophenone.

Fig. 3 details the results of the initial catalyst screening with 5 catalysts for activity for PE conversion and a control run with PE and no catalyst.

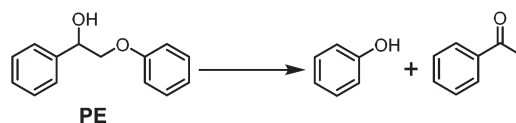


Fig. 2 The screening experiments with HTC catalysts result in base-catalysed β -O-4 bond cleavage in the model compound PE to produce phenol and acetophenone.

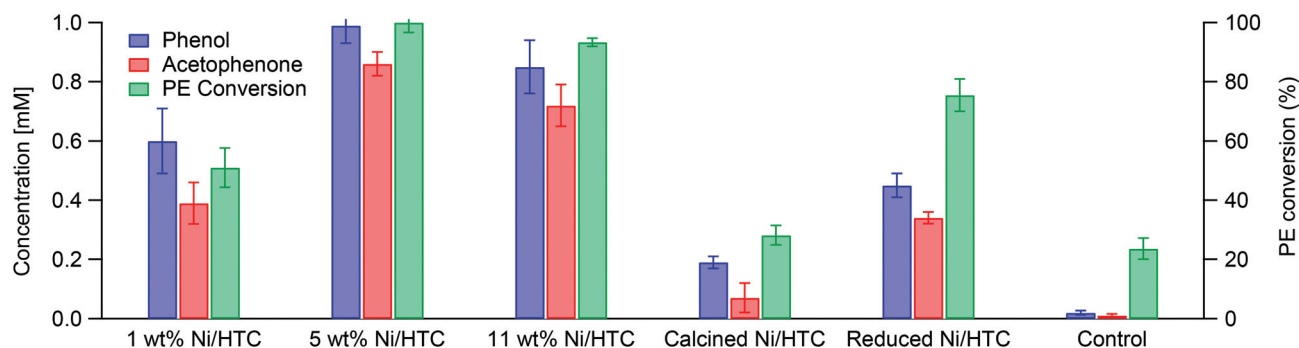


Fig. 3 Results of catalyst screening with PE at 270 °C for 1 h in MIBK.

Under these conditions, the as-prepared, loaded Ni/HTC catalysts are the most active in PE conversion. Lowering the nickel loading from 11 to 5 wt% has little effect, but the 1 wt% Ni/HTC exhibits a significant decrease in conversion from ~100 to 50%. Little conversion is observed in the control reaction. Modification of the 5 wt% Ni/HTC catalyst *via* calcination or reduction lowers the activity to 28% conversion and 75% conversion, respectively. It is known that heating HTC can thermally remove the interstitial hydroxide anions.⁶⁸ As the hydroxide anions are hypothesised to be an active catalytic species and calcining may remove these species, it is perhaps not surprising that the calcined catalyst exhibits lower activity.

Additionally, it is known that LDH catalysts promote aldol condensation.⁴² A common result of the experiments illustrated in Fig. 3 as well as subsequent figures reporting conversion data for PE on HTC catalysts is the lower yield of acetophenone relative to phenol. GC/MS results suggest that MIBK undergoes a small amount of cross-condensation with acetophenone, as well as self-condensation reactions in the presence of HTC catalysts (data not shown), hence the acetophenone yield is lower. Mass closures of 90% and EDS, ICP, and CHN analyses (Table S1 and Fig. S1†) indicate that very little product is lost due to charring during the reaction and that nickel leaching is negligible.

The results summarised in Fig. 3 demonstrate that 5 and 11 wt% nickel-supported HTC are effective catalysts for cleavage of the β -O-4 bond. To ascertain the catalytic properties responsible for aryl-ether bond cleavage, a series of additional experiments were performed in which HTC alone (the support material containing interstitial hydroxide anions), Ni(NO₃)₂ (the loaded nickel species), and a 5 wt% Ni/Al₂O₃ catalyst (a standard supported nickel catalyst) were investigated as catalysts with PE. NaOH was also employed to determine if base-catalysed cleavage produces the same reaction products. Results of these experiments are summarised in Fig. 4. HTC alone and Ni(NO₃)₂ are not active catalysts, exhibiting only 28% and 23% conversion of PE respectively. The 5 wt% Ni/Al₂O₃ exhibits low, partial conversion of 23%.

NaOH catalysis of PE in water produces the same product distribution as the HTC catalysed-reaction, and the yield of

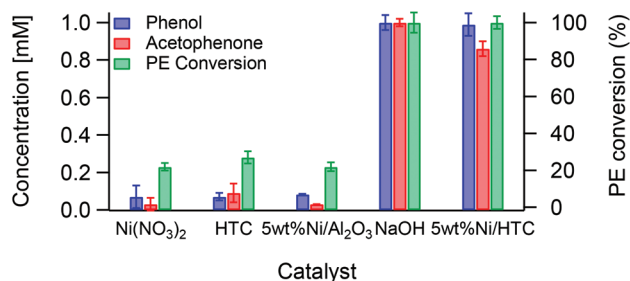


Fig. 4 Results of secondary screening to ascertain the catalytic properties responsible for aryl-ether bond cleavage. The Ni(NO₃)₂, HTC, and Ni/Al₂O₃ reactions were conducted at 270 °C for 1 h in MIBK. The NaOH experiments were conducted in deionised H₂O. The original 5 wt% Ni/HTC results are shown for reference.

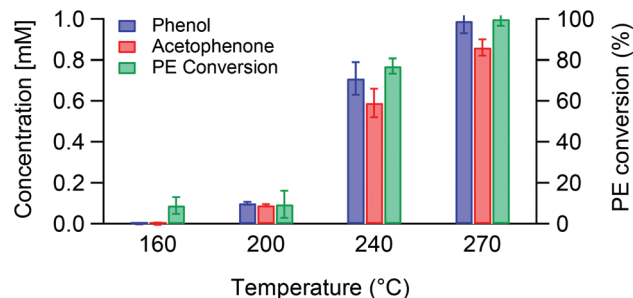


Fig. 5 Temperature effects on catalytic conversion of PE (5 wt% Ni/HTC, 1 h).

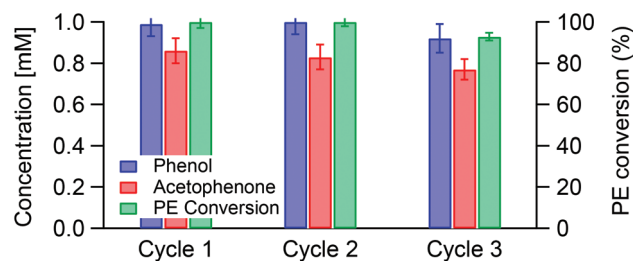


Fig. 6 Catalyst recycling study (5 wt% Ni/HTC, 270 °C, 1 h).

acetophenone and phenol are equal here, further suggesting that HTC promotes aldol condensation of acetophenone and MIBK. Taken together, these results suggest that Ni/HTC catalytic activity is not a result of the individual species, but rather a synergistic effect between supported nickel and HTC, and that the mechanism follows one similar to base-catalysed cleavage of PE.

Additionally, the effect of reaction temperature on PE conversion was studied using the 5 wt% Ni/HTC catalyst (Fig. 5). PE conversion activity precipitously drops off at 200 °C with the majority of activity still remaining at 240 °C. Activity was greatest at 270 °C, showing over 90% PE conversion.

Preliminary recycling studies show that the 5 wt% Ni/HTC catalyst maintains activity over 3 catalytic cycles (Fig. 6). Further recyclability studies are on-going currently with calcination/rehydration cycles for catalyst regeneration.

To determine if the 5 wt% Ni/HTC catalyst can degrade biomass-derived lignin, it was tested with lignin from two extraction processes: namely, lignin from an Organosolv process, Clean Fractionation (CF), at 270 °C for 1 h in MIBK and ball-milled lignin (BML) in water at 270 °C for 1 h in water.

Apparent molecular weights (MW) obtained by GPC are provided in Fig. 7. In both cases, a control reaction was also conducted in which the two lignin samples in the same solvents were heated to 270 °C to examine uncatalysed deconstruction of lignin. In Fig. 7A, the original CF lignin shows a large MW range from 300–10 000 Da. Upon heating in MIBK (“Control” in Fig. 7a), the CF lignin exhibits a shift to lower MW due to expected partial thermal decomposition (200–2000 Da) as would be observed in hydrothermal liquefaction. However the MW of

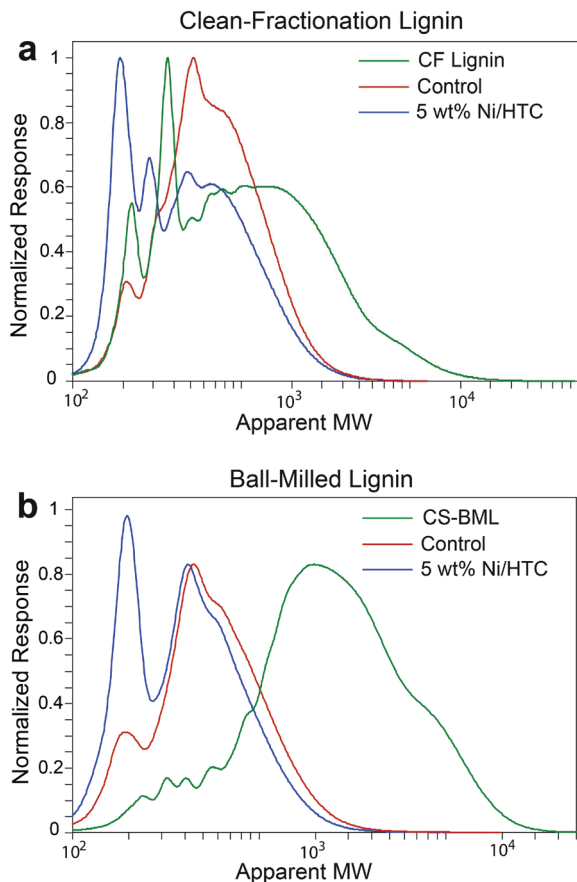


Fig. 7 GPC data from catalytic deconstruction of biomass-derived lignin. (a) Deconstruction of lignin from Clean Fractionation in MIBK. The green (CF lignin) curve shows the molecular weight distribution of the original lignin from an Organosolv process (Clean Fractionation). The red (Control) and blue (5 wt% Ni/HTC) show the molecular weight distributions after reaction (270 °C, 1 h) of thermal and catalytic deconstruction, respectively, of the CF lignin. (b) Deconstruction of ball-milled lignin in water. The green (CS-BML) curve shows the molecular weight distribution of the original lignin after ball milling. The red (Control) and blue (5 wt% Ni/HTC) show the molecular weight distributions after reaction (270 °C, 1 h) of thermal and catalytic deconstruction, respectively, of the BML.

the CF lignin run with the 5 wt% Ni/HTC catalyst in MIBK was substantially reduced, with a significant portion of material present as monomeric species below 200 Da (the GPC measurements for lignin are only semi-quantitative, and should primarily be interpreted as relative trends). Fig. 7B shows that the BML in water (“Control”) also undergoes partial thermal depolymerization, and the catalysed reaction produces a significant amount of low molecular-weight species.

Following catalysis, the lignin deconstruction products were examined in both the CF-lignin and BML substrates to identify the monomeric species produced catalytically. Fig. 8 shows the GC/MS chromatogram along with identified products. Monomeric species arising from CF-lignin include deconstruction products from both carbohydrates (furan containing compounds) as well as lignin sources (phenolic aromatic compounds). The lignin deconstruction products from the BML sample include products that arise from coumaryl, coniferyl, and

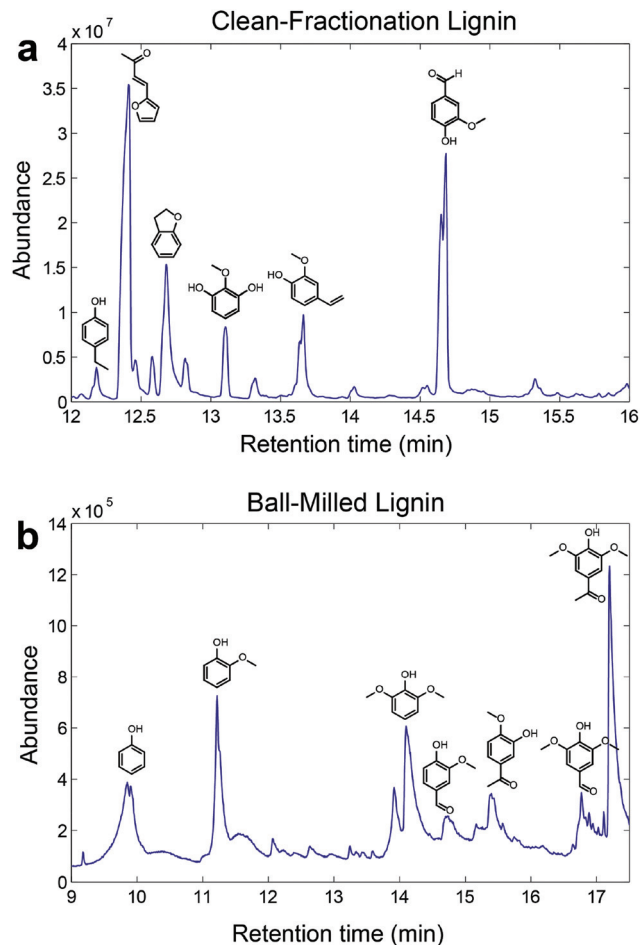


Fig. 8 Resulting product distribution from catalysis of biomass-derived lignin treated with the 5% Ni/HTC catalyst at 270 °C for 1 h determined by GC/MS. (A) Deconstruction products from CF lignin. (B) Deconstruction products from BML.

sinapyl sources (phenol, guaiacol, and syringol respectively).³⁰ All identified relevant peaks are listed in Table S2.† Both the GPC and GC/MS results indicate that the 5 wt% Ni/HTC catalyst is capable of breaking down lignin in biomass-derived feedstocks.

Catalyst characterisation

Interaction of the loaded nickel species with HTC and the fate of nickel in the 5 wt% Ni/HTC catalysts during reaction were studied before and after one PE conversion cycle (2 : 1 catalyst loading, 270 °C, 1 h) using several analytical methods including XRD, XPS, and SEM/EDS. A change in the colour of the catalyst was noted after reaction. The freshly prepared Ni/HTC catalyst is light green, and after reaction the catalyst is black. The XRD pattern of the catalyst (Fig. 9) indicates that nickel in the fresh catalyst (blue spectrum) is present as mainly Ni(OH)₂ rather than the loaded Ni(NO₃)₂ species. The prominent peak at 20° is from Ni(OH)₂, which arises from nickel interacting with the HTC support. The peak at 43.5° may also suggest the presence of nickel oxides. Previous researchers have attributed a similar peak to NiO, NiOOH, or Ni₂O₃, while other peaks for these compounds coincide with HTC or Ni(OH)₂.^{69–72} The XRD

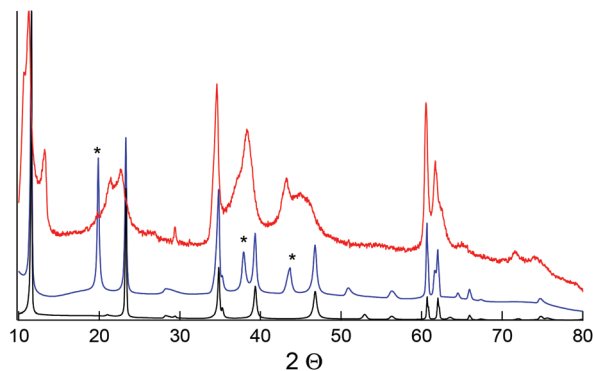


Fig. 9 XRD patterns of fresh 5 wt% Ni/HTC (blue, * peaks arising from Ni(OH)₂), used catalyst (red), and HTC (black).

pattern of the used catalyst shows that under the reaction conditions (270 °C), features from a dehydrated HTC structure arise, as seen in the shift of the (003) peak at 11.4° 2θ to a higher angle and broadening of the (009) peak at 35° 2θ.^{73,74} The peaks arising from Ni(OH)₂ species (2θ = 19.8°, 37.8°, and 43.5°) seen in the fresh catalyst shift for the used catalyst with the prominent peaks characterised as a mixed valence nickel oxide (2θ = 21.1°, 36.9°, and 43.0°). This seems to indicate that the Ni(OH)₂ species (which is green) is converted to the mixed valence nickel oxide during reaction (which in its oxygen rich, non-stoichiometric structure is black⁷²), and this hypothesis is confirmed by XPS as described below. As shown in Fig. 6, the recycling study indicates that the mixed valence nickel oxide species is still as active in PE conversion.

To gain further insight into the fate of nickel, XPS analysis was conducted on the same freshly prepared 5 wt% Ni/HTC catalyst as well as the 5 wt% Ni/HTC catalyst that had been used once for PE conversion (used catalyst) (Fig. 10). Generally, XPS spectra of supported nickel species are rather difficult to deconvolute, as several reports have assigned the peak envelope from 853.7 to 855.7 eV as a mixture of nickel oxides and Ni(OH)₂.^{59,75,76} XPS analysis of the fresh catalyst indicates that nickel is mainly present as Ni(OH)₂. The shape of Ni 2p spectrum of fresh catalyst (Fig. 10, blue line) closely resembles that of Ni(OH)₂, with the exception of small differences in the region corresponding to satellite structure, possibly due to presence of small amounts of Ni(NO₃)₂ as demonstrated by

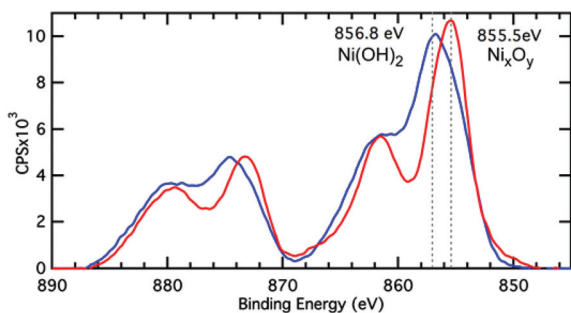


Fig. 10 Ni 2p XPS of fresh (blue) and used (red) 5 wt% Ni/HTC catalyst. "Ni_xO_y" in this graph is likely a mixed valence nickel oxide.

the asymmetry of the peak envelope centred at 856.8 eV. As XPS is quite sensitive to surface species, it is not surprising that Ni(NO₃)₂, which is not observed in XRD analysis, is present in the spectra. This Ni(OH)₂ species (confirmed in both XRD as well as XPS) is responsible for the light green colour of the freshly synthesised catalyst. The presence of Ni(OH)₂ in the XPS spectrum confirms that there is indeed an interaction when nickel is loaded onto the HTC support that will immediately convert some of the Ni(NO₃)₂ to Ni(OH)₂. Ni(OH)₂ is tightly bound to the support and is insoluble in both water as well as MIBK, as experimentally confirmed *via* hot water washes in which no nickel species were lost as indicated from SEM/EDS analysis (Table S1†). After reaction, the peak formerly centered at 856.8 eV has sharpened and shifted to a slightly lower energy of 855.5 eV, indicating that both Ni(NO₃)₂ (and likely Ni(OH)₂ as indicated by XRD) have converted to a mixed valence nickel oxide, which is responsible for the visually observed dark colour in the used catalyst. There are no changes in binding energy of 852–853 eV that would indicate appearance of Ni⁰, further indicating that changes in catalyst are due to conversion to nickel oxide species rather than reduction. This result is corroborated by the lower activity of the reduced catalyst shown in Fig. 3 relative to the high activity maintained over several runs by the mixed valence nickel oxide catalyst, as shown in Fig. 6.

SEM imaging provides insight as to why Ni/HTC is an active catalyst. HTC particles are on the order of tens of microns; however, the particles are agglomerates of nanoscale subunits, giving rise to a high surface area, macroporous network with pore diameters ranging from ~0.1–1 μm (Fig. 11). These pores are large relative to other catalysts, such as microporous zeolites, which are routinely used for conversion of petroleum-

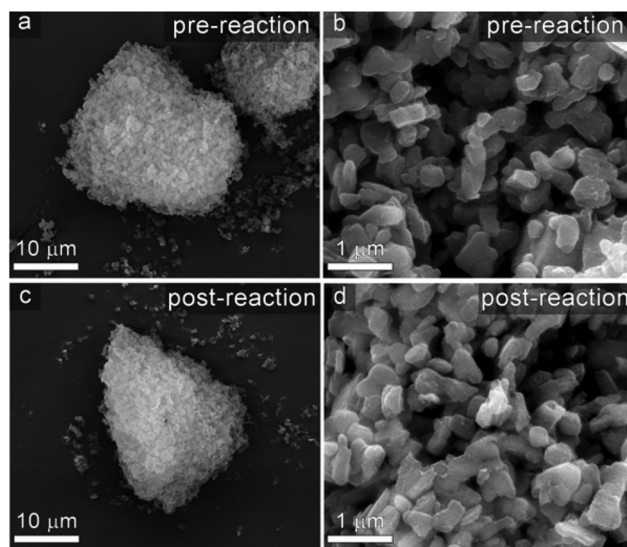


Fig. 11 Scanning electron microscopy of catalyst particles. The HTC-derived catalyst particles display porous, high-surface area micro- and nanoscale morphology. The microstructure of the catalyst particles is quite similar before and after the reaction. (a) Pre-reaction, 10 μm scale. (b) Pre-reaction, 1 μm scale. (c) Post-reaction, 10 μm scale. (d) Post-reaction, 1 μm scale.

based and biomass-derived small molecular weight species. The larger pore sizes displayed by the HTC catalysts used in this study are likely better suited to facilitate heterogeneous interaction with solubilised lignin polymers. Interestingly, no discernible changes to the catalyst microstructure were observed following chemical reaction (Fig. 11).

SEM imaging of fresh 5 wt% Ni/HTC shows that loading the nickel did not disrupt the highly porous substructure of the HTC support (Fig. 12a). The nanostructure of the catalysts was further investigated by TEM (Fig. 12b–d). These images illustrate that the individual nanoscale subunits of the larger catalyst particles are largely devoid of meso and micropores, and further supports that the macroporosity of the bulk catalyst particles is formed by the agglomeration of these constituents. An atomic layered structure of the catalyst may be observed in the high magnification image in Fig. 12d.

Elemental mapping of the catalyst particles revealed a largely uniform distribution of nickel throughout the catalyst at the microscale (Fig. 12h), with no evidence of phasing or localised clusters of nickel present at this scale. Interestingly, no loss of nickel from the catalyst support was detected after reaction by either EDS or ICP analysis (Table S1†), indicating that there was no metal leaching during the reaction. These results support the observation of a robust incorporation of nickel into the catalyst support that is resistant to leaching and structural degradation at the reaction conditions employed in this study. Similarly, ICP analysis of the PE solutions before and after reaction suggest very minor catalyst dissolution during reaction, yielding concentrations on the order of 1 mg L^{-1} Ni and 5 mg L^{-1} each Mg and Al (Fig. S1†). These concentrations correspond to 0.15% of the Ni and Mg and 0.42% of the Al in the catalyst, confirming the stability of the Ni component during reaction.

Discussion and conclusions

Lignin depolymerisation to low molecular weight species is a key step in lignin valorisation to fuels and chemicals. To date, many elegant studies have been conducted to examine homogeneous catalysts for selective cleavage of aryl–ether bonds, and many studies describe the development of solid catalysts for hydrogenolysis of biomass-derived lignin. For the latter case, these catalysts require reduced metals for activation of externally added hydrogen, which is then used to cleave inter-monomer linkages and to further deoxygenate lignin deconstruction products. Many of these systems utilise nickel as an active metal species for lignin depolymerisation, which has cost and abundance advantages over commonly used noble metals in hydrogen activation. In a different vein, the pulp and paper industry has a long history of lignin depolymerisation *via* homogeneous acid or basic catalysts such as Kraft and soda pulping. These depolymerisation processes with homogeneous acids and bases have been applied to isolated lignin at much harsher conditions with reasonable success to date for converting a substantial fraction of lignin to low molecular-weight species.

These two large bodies of literature on homogeneous alkaline catalysis and heterogeneous nickel-based catalysis of lignin motivated the work conducted here to combine nickel with a solid base support as a catalyst for lignin depolymerisation. The results of this study show that a 5 wt% Ni/HTC catalyst is quite active in the cleavage of a β -O-4 linkage in a lignin model compound, PE, as well as for the depolymerisation of two samples of biomass-derived lignin to small molecular-weight alkyl-aromatic species. Interestingly, the solid-base support, HTC, alone is not sufficiently active as prepared in this study to cleave the C–O bond in PE. With the addition of a

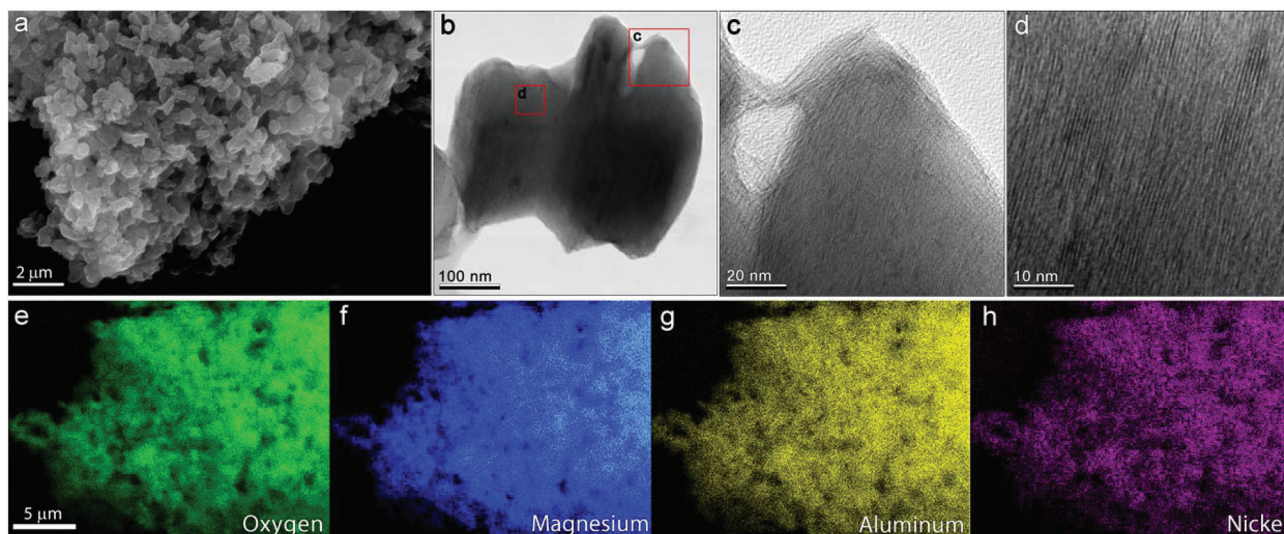


Fig. 12 Multiscale, multimodal imaging of 5 wt% Ni/HTC catalyst particles. (a) SEM imaging reveals the porous, high-surface area microscale morphology the catalyst particles. (b–d) TEM images of the nanostructure of an individual particle subunit. The atomic double-layer structure of the catalyst may be observed in the high-magnification image shown in (d). (e–h) EDS elemental analysis, performed in mapping mode, reveals the spatial distribution of elements within catalyst particles. These results show that that nickel is homogeneously distributed throughout the catalyst at the length scale of this analysis.

nickel salt, which converts to a mixed valence metal oxide upon heating, the catalyst becomes quite active for the desired transformation, and yields identical products to PE cleavage in NaOH (Fig. 2), suggesting a base-catalysed mechanism. Control experiments were employed to show that catalytic activity was a result of a synergistic effect between the nickel species with the HTC support (Fig. 4) with nickel present as a mixed valence nickel oxide (Fig. 10). Conversely to many heterogeneous catalysts for this purpose, the 5% Ni/HTC catalyst does not require a reduced metal nor external hydrogen for activity, thus generating a novel, effective catalyst for lignin depolymerisation at significantly lower severity than typically applied with metal catalysts. Moreover, the development of a solid-base catalyst offers a direct route to recycling compared to NaOH or other homogeneous catalysts.

Although the catalytic mechanism has not been fully elucidated, it is hypothesised that the nickel offers a strong binding site for the aryl ether bond of the lignin model compound or biomass-derived lignin polymer, and that the hydroxide anions in the catalyst interlayer are the active catalytic species. The mechanism will be elucidated in future studies with combined theoretical and experimental approaches, with additional characterisation work to ascertain the molecular state of nickel incorporation into the HTC structure in more detail. Additional work is also currently on going to further investigate deactivation and the impact of regeneration and recycling on LDH catalyst activity. Given the likely role of hydroxide anions for activity, the loss of oxygen from the catalyst measured by EDS, and the partial dehydration of the catalyst during the reaction cycle, regeneration in liquid water will likely be a viable strategy for this process as reported previously for LDH catalysts for other applications,⁷⁷ which will be reported in a forthcoming study.

In summary, the Ni/HTC catalyst offers a potentially viable alternative to metal-catalysed hydrogenolysis or homogeneous catalysis of lignin. More generally, the durability of this catalyst system overall in terms of metal retention, ease of preparation, and temperature stability suggests that it may be viable for a broad range of solvent systems, operating conditions, and catalytic chemistries for applications in biomass conversion.

Experimental methods

Materials

All solvents: acetone (HPLC grade, Fisher), ethanol (200 proof Pharmco-AAPER), methanol (lab grade, Fisher), diethyl ether (99.5%, Fisher), and methyl isobutyl ketone (reagent grade, Fisher) were used as received. 2-Bromoacetophenone, phenol, potassium carbonate, potassium iodide, sodium borohydride, magnesium sulphate, nickel nitrate, and hydrotalcite were all purchased from Sigma-Aldrich and used as received.

Model compound synthesis

2-Phenoxy-1-phenylethanol (PE) was synthesised in accordance with Nichols *et al.*¹⁸ Step 1: 2-phenoxy-1-phenylethanol was

synthesised in the following manner: a round bottom flask equipped with a reflux condenser was charged with 2-bromoacetophenone (11.9424 g, 60 mmol), phenol (7.0582 g, 75 mmol), K₂CO₃ (12.3000 g, 89 mmol), KI (catalytic) and acetone (250 mL). The resulting mixture was heated to reflux and allowed to react for 3 h, after which it was filtered and concentrated. 2-Phenoxy-1-phenylethanol was crystallised from cold ethanol (250 mL) (85% yield). Step 2: 2-phenoxy-1-phenylethanol (1.1089 g, 5.2 mmol) was dissolved in 35 mL of methanol. Sodium borohydride (0.3534 g, 10.4 mmol) was added portion-wise generating a gentle evolution of gas, after which the reaction mixture was stirred at room temperature for 2 h. The reaction was quenched with a saturated aqueous NH₄Cl solution (30 mL). The resultant mixture was extracted with 20 mL diethyl ether three times. The combined organic extracts were dried with 50 mL saturated brine solution, dried over MgSO₄, and filtered. The filtrate was evaporated to dryness to afford an off-white solid of 2-phenoxy-1-phenylethanol (80% yield). The solid was dried overnight in a vacuum desiccator.

Catalyst synthesis

The catalysts used in this study were prepared in the following manner: based on the desired weight loading, a solution of Ni(NO₃)₂·6H₂O in absolute ethanol was combined with the hydrotalcite support with constant stirring and this mixture was then left on a heating plate, at 25 °C, to dry completely overnight. EA of 5 wt% Ni/HTC gave Al 10.46 wt%, Mg 17.36 wt%, and Ni 4.44 wt%. Unless specified, catalysts were used as synthesised without modification.

Catalyst screening methods

Catalysts were screened *via* a heated batch reaction method. Catalysts were loaded into 3 mL stainless steel batch reactors and charged with 3 mL of stock solution giving PE substrate to catalyst loading of 1 : 2. Experiments were run in triplicate. The reactors were tightly sealed and submerged in a heated temperature-controlled sand bath. Temperature was monitored with a thermal couple. After a designated time the reactors were removed from the sand bath and the reaction was quenched immediately by inserting the reactors into an ice bath.

In the post reaction work up of products, the reactors were opened and the contents were centrifuged to collect the used catalyst. This catalyst was then washed with acetone, centrifuged, and left to dry for further analysis. The resulting solution was then brought up to a final volume of 10 mL with acetone. For the subsequent GC analysis, the products were diluted 10 times to bring final concentrations into calibrated range of 0–1 mM with a 1.0 mM durenene internal standard. Samples were analysed in an Agilent Technologies 7890A GC equipped with an FID detector employing an HP-5MS column (30 m × 0.25 mm × film thickness 0.25 μm, Agilent Technologies). The temperature program was as follows: 45 °C hold for 3 min; ramp to 200 at 15 °C min⁻¹ hold for 6 min; total run time of 19.33 min. In all cases mass closures (based

on conversion and production of phenol) were greater than 90%.

Clean fractionation procedures

Fractionation of corn stover was carried out as follows: whole corn stover (10 g) in a single-phase mixture of MIBK–acetone–H₂O (11/44/44 wt%, 100 mL) with sulphuric acid (0.1 M) was loaded into a Hastelloy pressure reactor. The reactor was sealed and heated in an electric heating block at 140 °C for 56 min. After the reaction, the reactor was cooled in ice water. Reaction mixture was filtrated and the residual solid was washed with the same solvent (200 mL) and deionised H₂O (650 mL) to remove the soluble fraction completely. The combined black filtrate (MIBK–acetone–H₂O) was mixed in a separatory funnel, shaken, and allowed to stand for 1 hour to separate the aqueous and organic phases. The aqueous layer was extracted with MIBK (25 mL). MIBK layers were combined, washed with deionised H₂O, evaporated to remove volatiles, and dried in a vacuum oven at 35 °C for 4 days to obtain the lignin-enriched fraction.

Ball-milled lignin preparation

Ball-milled lignin (BML) was prepared from extractives-free corn stover according to the Björkman method.³¹ Corn stover was extracted with water and ethanol for 48 hours, respectively, using a soxhlet extractor. Air-dried extractives-free corn stover was ground in toluene at 4 °C for 2 weeks, in ceramic jars (0.3 L volume) using ceramic balls under a nitrogen atmosphere. Ball-milled corn stover (1096 g) was extracted with 1.5 L of 96% dioxane (v/v) for 2 days with vigorous stirring. The suspension was filtered and solid residue was extracted with same solvent for additional 2 days. Combined filtrate was evaporated at 40 °C under reduced pressure to obtain crude BML (31.3 g). The crude BML was dissolved in 90% acetic acid and precipitated into water. The precipitate was collected by centrifugation and then washed with water 3 times until acetic acid was removed. Freeze dried precipitate was dissolved into 85 mL of 1,2-dichloroethane–ethanol (2 : 1, v/v) and precipitating into diethyl ether (800 mL). The precipitate was recovered by centrifugation (18 000 rpm, 10 min) and then washed with ether 2 times to obtain corn stover BML (14.4 g, 1.32 wt%). The lignin and carbohydrate contents in the BML were 84.4 and 7.51 wt%, respectively.

Gel permeation chromatography (GPC) analysis

After the catalytic deconstruction of biomass derived lignin samples (20 mg), the reaction mixture and wash solvent (10 mL of acetone) was filtrated through a 0.2 µm nylon membrane syringe filter. The filtrate was concentrated to approximately 2 mL using a gentle stream of nitrogen gas. The deconstruction mixture was acetylated in a mixture of pyridine (0.5 mL) and acetic anhydride (0.5 mL) at 35 °C for 24 h with stirring. The reaction of acetylation was terminated by addition of methanol (0.2 mL) to neutralise the acetic anhydride. The acetylation solvents were then evaporated from the samples at 40 °C under a stream of N₂. The samples were further dried in

a vacuum oven at 40 °C overnight. The dried acetylated deconstruction products were dissolved in tetrahydrofuran (THF, Baker HPLC grade) to a final concentration of 2 mg mL⁻¹. The dissolved samples were filtered (0.45 µm nylon membrane syringe filters) before GPC analysis. The acetylated samples appeared to be completely soluble in THF. GPC analysis was performed using an Agilent HPLC with 3 GPC columns (Polymer Laboratories, 300 × 7.5 mm) packed with polystyrene-divinyl benzene copolymer gel (10 µm beads) having nominal pore diameters of 10⁴, 10³, and 10² Å. The eluent was THF and the flow rate was 1.0 mL min⁻¹. An injection volume of 25 µL was used. The HPLC was attached to a diode array detector measuring absorbance at 260 nm (band width 40 nm). Retention time was converted into molecular weight by applying a calibration curve established using polystyrene standards.

GC/MS characterization of lignin deconstruction products

Analysis of samples was performed on an Agilent 7890 GC equipped with a 5975 MS (Agilent Technologies, Palo Alto, CA). Sample compounds were separated using a 30 m × 0.25 mm × 0.25 µm HP-5MS column (Agilent). HP MSD Chemstation software (Agilent) equipped with NIST11 database Rev. 2.0G (May 19, 2011 build) was used to determine the identity of the unknown compounds found within the samples. Each sample was placed on an auto-sampler (Agilent) and injected at a volume of 1 µL into the GC/MS (Agilent). The GC/MS method consisted of a front inlet temperature of 280 °C, MS transfer line temperature of 280 °C, and a scan range from 35 *m/z* to 550 *m/z*. A starting temperature of 35 °C was held for 5 minutes and then ramped at 15 °C min⁻¹ to a temperature of 225 °C with no hold time, then continued at a ramped rate of 15 °C min⁻¹ to 300 °C and held for 4 minutes. The method resulted in a run time of 27 minutes for each sample. No standards were added for the purpose of quantification.

Catalyst characterisation procedures

X-Ray diffraction. XRD was conducted on powdered samples using a Rigaku Ultima IV diffractometer with a Cu K α radiation source (40 kV and 44 mA). Scans were collected from 10–80° 2 θ with a step size of 0.01° using a dTex detector. Diffraction data were processed using Rigaku PDXL software, and peaks were matched against the International Centre for Diffraction Data (ICDD) database PDF 2009.

X-Ray photoelectron spectroscopy. XPS analysis was performed using a Physical Electronics PE5600 XPS system. Samples were pressed into indium foil. Spectra were collected using a monochromatic Al K α X-ray source operated at 350 W, hemispherical analyser, and multichannel detector. A low-energy (~1 eV) electron flood gun was used for charge neutralisation. Survey spectra were collected using an analyser pass energy and step size of 187.85 eV and 0.8 eV per step, respectively. High-resolution spectra were collected using an analyser pass energy of 23.50 eV and a step size of 0.1 eV per step. The quantification was performed using the default relative sensitivity factor (RSF) values supplied by the XPS

manufacturer. Data analysis was performed using CasaXPS software (<http://www.casaxps.com>). A linear background was applied to C 1s, O 1s and N 1s spectra and Shirley background was used for Ni 2p and Mg 1s spectra. High-resolution spectra were charge referenced by setting the C 1s hydrocarbon peak to 284.8 eV.

Scanning electron microscopy. SEM was performed using a FEI Quanta 400 FEG instrument. Samples were mounted on aluminum stubs with conductive carbon tape adhesive and sputter-coated with 7 nm of iridium prior to imaging. Images were obtained at an accelerating voltage of 30 keV.

Energy dispersive X-ray spectroscopy. EDS was performed in the aforementioned SEM instrument equipped with an EDAX X-ray detector using the same sample preparation methods used for SEM imaging. Elemental composition was obtained from at least 5 EDS spectra collected at each experimental condition; spectra were quantified using an atomic number (ZAF) correction. EDS mapping was performed in Quant mode based on net intensity using dwell time of 200 ms per pixel.

Inductively coupled plasma-atomic emission spectroscopy. Solid samples of 25 mg were dissolved in 10 mL concentrated HNO₃ (69.5%, KMG company) and heated in a microwave oven from room temperature to 200 °C over 5 minutes and then held at 200 °C for 10 minutes. After cooling to room temperature, the contents were washed out of the vessels, filtered through a glass filter and diluted to a volume of 50 mL. Liquid samples (3 mL) of 33 mM PE in MIBK before and after reaction were diluted to 10 mL with acetone, then evaporated to a non-volatile residue. The residue was dissolved in a solution of 2 mL concentrated HNO₃ and 8 mL of deionised water and analysed directly. Analyses were performed on a Spectro Arcos FHS12 at a plasma power of 1425 W. The instrument was calibrated by dilution of commercial standards with the same nitric acid solution used to dilute samples (20 vol% concentrated nitric acid in deionized water). Samples were analyzed for Ni at 231.6 nm, Al at 167.1 nm and Mg at 279.6 nm.

Transmission electron microscopy. Catalyst particles were suspended in ethanol and drop-cast onto carbon coated, 200 mesh copper grids (SPI Supplies, West Chester, PA). Grids were allowed to air dry and images were captured with a four mega-pixel Gatan UltraScan 1000 camera (Gatan, Pleasanton, CA) on a FEI Tecnai G2 20 Twin 200 kV LaB6 TEM (FEI, Hillsboro, OR).

Acknowledgements

We acknowledge funding from the National Advanced Biofuels Consortium, funded by the US Department of Energy (DOE) BioEnergy Technologies Office (BETO) through Recovery Act Funds, the US DOE BETO, the NREL Laboratory Directed Research and Development Program, and the Center for Direct Catalytic Conversion of Biomass to Biofuels (C3Bio), an Energy Frontier Research Center funded by the U.S. DOE, Office of

Science, Office of Basic Energy Sciences, Award Number DE-SC0000997. We thank David Johnson for conducting the GPC measurements, Joel Pankow and Svitlana Pylypenko for collecting and analysing XPS data, and Jessica Olstad for performing the ICP and CHN analyses.

Notes and references

- 1 Y. Pu, F. Hu, F. Huang, B. Davison and A. Ragauskas, *Bio-technol. Biofuels*, 2013, **6**, 15.
- 2 W. Boerjan, J. Ralph and M. Baucher, *Annu. Rev. Plant Biol.*, 2003, **54**, 519–546.
- 3 N. D. Bonawitz and C. Chapple, in *Annual Review of Genetics*, ed. A. Campbell, M. Lichten and G. Schupbach, Annual Reviews, Palo Alto, 2010, vol. 44, pp. 337–363.
- 4 M. C. McCann and N. C. Carpita, *Curr. Opin. Plant Biol.*, 2008, **11**, 314–320.
- 5 S. Kim, S. C. Chmely, M. R. Nimos, Y. J. Bomble, T. D. Foust, R. S. Paton and G. T. Beckham, *J. Phys. Chem. Lett.*, 2011, **2**, 2846–2852.
- 6 D. M. Alonso, S. G. Wettstein and J. A. Dumesic, *Chem. Soc. Rev.*, 2012, **41**, 8075–8098.
- 7 R. Parthasarathi, R. A. Romero, A. Redondo and S. Gnanakaran, *J. Phys. Chem. Lett.*, 2011, **2**, 2660–2666.
- 8 S. P. S. Chundawat, G. T. Beckham, M. E. Himmel and B. E. Dale, in *Annual Review of Chemical and Biomolecular Engineering*, ed. J. M. Prausnitz, Annual Reviews, Palo Alto, 2011, vol. 2, pp. 121–145.
- 9 J. Holladay, J. Bozell, J. White and D. Johnson, *Top value-added chemicals from biomass volume II—results of screening for potential candidates from biorefinery lignin*, Pacific Northwest National Laboratory, Oak Ridge, TN, USA, 2007.
- 10 J. Shabtai, W. Zmierzak and E. Chornet, Conversion of lignin to reformulated gasoline compositions. 1. Basic processing scheme, 1997.
- 11 J. Shabtai, W. Zmierzak, E. Chornet and D. K. Johnson, *Prepr. Symp. - Am. Chem. Soc., Div. Fuel Chem.*, 1999, **44**, 267–272.
- 12 J. Shabtai, W. Zmierzak, E. Chornet and D. K. Johnson, Conversion of lignin. 2. Production of high-octane fuel additives, 1999.
- 13 J. Shabtai, W. Zmierzak, S. Kadangode, E. Chornet and D. K. Johnson, Lignin conversion to high-octane fuel additives, 1999.
- 14 J. S. Shabtai, W. W. Zmierzak and E. Chornet, WO9910450A1, 1999.
- 15 A. Vigneault, D. K. Johnson and E. Chornet, *Can. J. Chem. Eng.*, 2007, **85**, 906–916.
- 16 J. E. Miller, L. Evans, A. Littlewolf and D. E. Trudell, *Fuel*, 1999, **78**, 1363–1366.
- 17 V. M. Roberts, V. Stein, T. Reiner, A. Lemonidou, X. B. Li and J. A. Lercher, *Chem.-Eur. J.*, 2011, **17**, 5939–5948.
- 18 J. M. Nichols, L. M. Bishop, R. G. Bergman and J. A. Ellman, *J. Am. Chem. Soc.*, 2010, **132**, 12554–12555.

- 19 S. C. Chmely, S. Kim, P. N. Ciesielski, G. Jimenez-Oses, R. S. Paton and G. T. Beckham, *ACS Catal.*, 2013, **3**, 963–974.
- 20 A. Wu, B. O. Patrick, E. Chung and B. R. James, *Dalton Trans.*, 2012, **41**, 11093–11106.
- 21 S. K. Hanson, R. T. Baker, J. C. Gordon, B. L. Scott and D. L. Thorn, *Inorg. Chem.*, 2010, **49**, 5611–5618.
- 22 S. K. Hanson, R. L. Wu and L. A. Silks, *Angew. Chem., Int. Ed.*, 2012, **51**, 3410–3413.
- 23 B. Sedai, C. Diaz-Urrutia, R. T. Baker, R. L. Wu, L. A. Silks and S. K. Hanson, *ACS Catal.*, 2011, **1**, 794–804.
- 24 T. Elder and J. J. Bozell, *Holzforschung*, 1996, **50**, 24–30.
- 25 T. Elder, J. J. Bozell and D. Cedeno, *Phys. Chem. Chem. Phys.*, 2013, **15**, 7328–7337.
- 26 J. Zakzeski, A. L. Jongerius and B. M. Weckhuysen, *Green Chem.*, 2010, **12**, 1225–1236.
- 27 B. Biannic and J. J. Bozell, *Org. Lett.*, 2013, **15**, 2730–2733.
- 28 P. Kelley, S. B. Lin, G. Edouard, M. W. Day and T. Agapie, *J. Am. Chem. Soc.*, 2012, **134**, 5480–5483.
- 29 A. G. Sergeev and J. F. Hartwig, *Science*, 2011, **332**, 439–443.
- 30 J. Zakzeski, P. C. A. Bruijninx, A. L. Jongerius and B. M. Weckhuysen, *Chem. Rev.*, 2010, **110**, 3552–3599.
- 31 M. P. Pandey and C. S. Kim, *Chem. Eng. Technol.*, 2011, **34**, 29–41.
- 32 T. H. Parsell, B. C. Owen, I. Klein, T. M. Jarrell, C. L. Marcum, L. J. Hauptert, L. M. Amundson, H. I. Kenttaemaa, F. Ribeiro, J. T. Miller and M. M. Abu-Omar, *Chem. Sci.*, 2013, **4**, 806–813.
- 33 X. Y. Wang and R. Rinaldi, *ChemSusChem*, 2012, **5**, 1455–1466.
- 34 A. G. Sergeev, J. D. Webb and J. F. Hartwig, *J. Am. Chem. Soc.*, 2012, **134**, 20226–20229.
- 35 P. Azadi, O. R. Inderwildi, R. Farnood and D. A. King, *Renew. Sustainable Energy Rev.*, 2013, **21**, 506–523.
- 36 Y. Matsumura, M. Sasaki, K. Okuda, S. Takami, S. Ohara, M. Umetsu and T. Adschiri, *Combust. Sci. Technol.*, 2006, **178**, 509–536.
- 37 K. Okuda, X. Man, M. Umetsu, S. Takami and T. Adschiri, *J. Phys.: Condens. Matter*, 2004, **16**, S1325–S1330.
- 38 Z. Tang, Y. Zhang and Q. Guo, *Ind. Eng. Chem. Res.*, 2010, **49**, 2040–2046.
- 39 Q. Song, F. Wang, J. Cai, Y. Wang, J. Zhang, W. Yu and J. Xu, *Energy Environ. Sci.*, 2013, **6**, 994–1007.
- 40 J. C. Hicks, *J. Phys. Chem. Lett.*, 2011, **2**, 2280–2287.
- 41 R. Rinaldi and F. Schuth, *Energy Environ. Sci.*, 2009, **2**, 610–626.
- 42 D. P. Debecker, E. M. Gaigneaux and G. Busca, *Chem.–Eur. J.*, 2009, **15**, 3920–3935.
- 43 J. L. Shumaker, C. Crofcheck, S. A. Tackett, E. Santillan-Jimenez, T. Morgan, Y. Ji, M. Crocker and T. J. Toops, *Appl. Catal., B*, 2008, **82**, 120–130.
- 44 J. I. Di Cosimo, V. K. Diez, M. Xu, E. Iglesia and C. R. Apesteguia, *J. Catal.*, 1998, **178**, 499–510.
- 45 D. Tichit and B. Coq, *CATTECH*, 2003, **7**, 206–217.
- 46 D. Tichit, C. Gerardin, R. Durand and B. Coq, *Top. Catal.*, 2006, **39**, 89–96.
- 47 G. S. Macala, T. D. Matson, C. L. Johnson, R. S. Lewis, A. V. Iretskii and P. C. Ford, *ChemSusChem*, 2009, **2**, 215–217.
- 48 H. Liu, W. Xu, X. Liu, Y. Guo, Y. Guo, G. Lu and Y. Wang, *Kinet. Catal.*, 2010, **51**, 75–80.
- 49 Q. Wang and D. O'Hare, *Chem. Rev.*, 2012, **112**, 4124–4155.
- 50 Y. Liu, E. Lotero, J. G. Goodwin Jr. and X. Mo, *Appl. Catal., A*, 2007, **331**, 138–148.
- 51 A. Corma, S. Iborra, J. Primo and F. Rey, *Appl. Catal., A*, 1994, **114**, 215–225.
- 52 M. J. Climent, A. Corma, S. Iborra, K. Epping and A. Velty, *J. Catal.*, 2004, **225**, 316–326.
- 53 S. Abello, S. Dhir, G. Colet and J. Perez-Ramirez, *Appl. Catal., A*, 2007, **325**, 121–129.
- 54 S. Abello, F. Medina, D. Tichit, J. Perez-Ramirez, J. E. Sueiras, P. Salagre and Y. Cesteros, *Appl. Catal., B*, 2007, **70**, 577–584.
- 55 B. M. Choudary, M. L. Kantam, A. Rahman, C. V. Reddy and K. K. Rao, *Angew. Chem., Int. Ed.*, 2001, **40**, 763–766.
- 56 K. Takehira, T. Kawabata, S. Shishido, K. Murakami, T. Ohi, D. Shoro, M. Honda and K. Takaki, *J. Catal.*, 2005, **231**, 92–104.
- 57 C. Resini, T. Montanari, L. Barattini, G. Ramis, G. Busca, S. Presto, P. Riani, R. Marazza, M. Sisani, F. Marmottini and U. Costantino, *Appl. Catal., A*, 2009, **355**, 83–93.
- 58 C. M. Jinesh, C. A. Antonyraj and S. Kannan, *Catal. Today*, 2009, **141**, 176–181.
- 59 K. B. H. Finch, R. M. Richards, A. Richel, A. V. Medvedovici, N. G. Gheorghie, M. Verziu, S. M. Coman and V. I. Parvulescu, *Catal. Today*, 2012, **196**, 3–10.
- 60 S. Narayanan and K. Krishna, *Appl. Catal., A*, 1996, **147**, L253–L258.
- 61 S. Narayanan and K. Krishna, *Appl. Catal., A*, 1998, **174**, 221–229.
- 62 S. Narayanan and K. Krishna, *Appl. Catal., A*, 2000, **198**, 13–21.
- 63 A. Takagaki, M. Takahashi, S. Nishimura and K. Ebitani, *ACS Catal.*, 2011, **1**, 1562–1565.
- 64 Z. Strassberger, A. H. Alberts, M. J. Louwerse, S. Tanase and G. Rothenberg, *Green Chem.*, 2013, **15**, 768–774.
- 65 M. Ni, D. Y. C. Leung and M. K. H. Leung, *Int. J. Hydrogen Energy*, 2007, **32**, 3238–3247.
- 66 J. Comas, F. Marino, M. Laborde and N. Amadeo, *Chem. Eng. J.*, 2004, **98**, 61–68.
- 67 J. J. Bozell, S. K. Black, M. Myers, D. Cahill, W. P. Miller and S. Park, *Biomass Bioenergy*, 2011, **35**, 4197–4208.
- 68 J. Zhang, Y. F. Xu, G. Qian, Z. P. Xu, C. Chen and Q. Liu, *J. Phys. Chem. C*, 2010, **114**, 10768–10774.
- 69 Z. Jiang, R. Song, W. Bi, J. Lu and T. Tang, *Carbon*, 2007, **45**, 449–458.
- 70 F. Bardé, M. R. Palacín, B. Beaudoin, P. A. Christian and J. M. Tarascon, *J. Power Sources*, 2006, **160**, 733–743.
- 71 G. Fan, X. Xiang, J. Fan and F. Li, *J. Mater. Chem.*, 2010, **20**, 7378–7385.
- 72 M. A. Vidales-Hurtado and A. Mendoza-Galván, *Mater. Chem. Phys.*, 2008, **107**, 33–38.

- 73 E. Kanezaki, *Inorg. Chem.*, 1998, **37**, 2588–2590.
- 74 J. Perez-Ramirez, S. Abello and N. M. van der Pers, *Chem.–Eur. J.*, 2007, **13**, 870–878.
- 75 M. C. Biesinger, B. P. Payne, L. W. M. Lau, A. Gerson and R. S. C. Smart, *Surf. Interface Anal.*, 2009, **41**, 324–332.
- 76 D. Addari, A. Mignani, E. Scavetta, D. Tonelli and A. Rossi, *Surf. Interface Anal.*, 2011, **43**, 816–822.
- 77 S. Abello, F. Medina, D. Tichit, J. Perez-Ramirez, J. C. Groen, J. E. Sueiras, P. Salagre and Y. Cesteros, *Chem.–Eur. J.*, 2005, **11**, 728–739.